LUMENAL PLASMA MEMBRANE OF THE URINARY BLADDER

I. Three-Dimensional Reconstruction from Freeze-Etch Images

L. ANDREW STAEHELIN, FRANCIS J. CHLAPOWSKI, and MARY A. BONNEVILLE

From the Biological Laboratories, Harvard University, Cambridge, Massachusetts 02138; the Department of Molecular, Cellular, and Developmental Biology, University of Colorado, Boulder, Colorado 80302; and the Department of Anatomy, University of Massachusetts Medical School, Worcester, Massachusetts 01604

ABSTRACT

To determine the three-dimensional structure of the lumenal membrane of transitional epithelium, a study was made of sectioned, negatively stained, and freeze-etched specimens from intact epithelium and membrane fractions from rabbit urinary bladder. Particulate membrane components are confined to plaque regions within which the unit membrane is asymmetric, having a thicker outer leaflet. Transversely fractured freeze-etched plaques display a thick (~80 A), particulate lumenal leaflet and a thin (~40 A) cytoplasmic one. Four different faces of the two leaflets can be distinguished: two complementary, split, inner membrane faces exposed by freeze-cleaving the bilayer and two external (lumenal and cytoplasmic) membrane surfaces revealed by deep-etching. On the split, inner face of the lumenal leaflet appear polygonal plaques of hexagonally arranged particles. These fit into holes observed on the complementary, split, innerface of the cytoplasmic leaflet. The particles, which have a center-to-center spacing of ~160 A, also seem to protrude from the external surface of the lumenal leaflet, where their subunits (~50 A in diameter) are revealed by freeze-etching and negative staining. The plaques are separated from each other by smooth-surfaced regions, which cleave like simple lipid bilayers. Since the array of plaque particles covers only ~73% of the membrane surface area, whereas 27% is taken up by particle-free interplaque regions, the presence of particles cannot in itself entirely account for the permeability barrier of the lumenal membrane. Although no particles are observed protruding from the cytoplasmic surface of the membrane, cytoplasmic filaments are attached to it by short, cross-bridge–like filaments that seem to contact the particles within the membrane. These long cytoplasmic filaments cross-link adjacent plaques. Therefore, we suggest that at least one function of the particles is to serve as anchoring sites for cytoplasmic filaments, which limit the expansion of the lumenal membrane during distention of the bladder, thereby preventing it from rupturing. The particle-free interplaque regions probably function as hinge areas between the stiff plaques, allowing the membrane to fold up when the bladder is contracted.

INTRODUCTION

The plasma membrane at the lumenal surface of the mammalian transitional epithelium is unique in its structure. This membrane, which is exposed to urine stored in the bladder, possesses concave

plaques of extraordinarily thick membrane (120 A) alternating with interplaque membrane of more usual thickness, namely 80 A (7, 19, 20, 21). This structure imparts a scalloped appearance to profiles seen in sectioned material. The significance of this structure is not clear, but it has generally been thought to correlate with the apparently complete impermeability of the membrane by which exchanges between hypertonic urine and the adjacent tissues are prevented.

Closer observations have revealed that the membrane of the plaques is asymmetrical, having a thin electron-opaque leaflet adjacent to the cytoplasm and a thick electron-opaque leaflet exposed to the lumen (7). When sectioned normally, the lumenal leaflet appears to be composed of uniformly spaced particles, and in tangential sections a faint hexagonal pattern may be seen (21). Experiments with negatively stained, isolated membranes indicate that the individual membrane-associated particles consist of hexagonally arranged subunits (10, 11, 24).

The distribution of particles on the membrane is of particular interest because Hicks (8) has suggested that they are composed of keratin and therefore constitute the chief permeability barrier. In order to be effective, the particles would seemingly have to be distributed over the entire lumenal membrane; but conflicting reports have been published regarding their disposition on the membrane. Observations on sectioned material (21) indicate that the characteristic pattern can be detected only in the plaque regions, where the lumenal membrane is thickened and asymmetrical in profile. Interplaque regions, however, appear to be free of particles. On the other hand, Hicks and Ketterer (10, 11) have reported that the hexagonal particles cover the whole membrane surface, as judged by negative staining.

Another interesting characteristic of the membrane is its ability to fold when the surface area of the epithelium decreases as the bladder contracts upon emptying. The folding apparently occurs in the interplaque regions (16, 20, 21) and may be related to a process of membrane turnover (9, 21). Information on the structure of the interplaque regions of the membrane is conspicuously lacking in spite of their obvious importance.

In this investigation, intact and homogenate fractions of lumenal plasma membranes of transitional epithelium from rabbit urinary bladders were examined by electron microscopy. By correlating the results obtained from sectioned material, negatively stained specimens, and freeze-etch replicas, we have attempted to: (*a*) resolve the controversy regarding the distribution of membrane particles; (*b*) define, more exactly, the relationship of the particles to other components of the membrane; and (*c*) obtain information on the structure of the interplaque membrane with the aim of understanding its role in the folding that occurs during contraction and distention of the bladder.

Portions of this work have been reported briefly (23).

MATERIALS AND METHODS

Preparation of Intact Bladders

Adult, female rabbits obtained from Charles River Breeding Laboratories, Inc., Wilmington, Mass., were anesthetized with intravenous injections of sodium pentobarbital (Nembutal, Abbott Laboratories Ltd., Queenborough, Kent, England). The urinary bladder was exposed *in situ* and the urethral end was clamped with a hemostat. The urine was withdrawn by means of a 50 ml syringe with an 18 gauge needle and replaced simultaneously with fixative injected by a second similar syringe. Care was taken to maintain the bladders in their naturally occurring state of distention or contraction by injecting and withdrawing fluids at a constant rate. At the same time, fixative was applied to the external surface of the bladder. After 10 min, pieces of the bladder wall were cut with fine scissors, transferred to a drop of fixative, cut with razor blades into small blocks ($\sim$1 mm^2), and placed in fresh fixative until the total desired period for fixation had elapsed.

Tissues were fixed for 2 hr in Karnovsky's (13) paraformaldehyde-glutaraldehyde mixture in 0.1 M cacodylate buffer (pH 7.4), rinsed overnight in the same buffer with 10% sucrose added, postfixed for 45 min in 1.33% osmium tetroxide buffered by *s*-collidine (pH 7.2), and stained en bloc with uranyl acetate (14). After dehydration in alcohols, specimens were embedded in Epon (17).

Sections were cut with a diamond knife on a Porter Blum MT-1 ultramicrotome, mounted on copper grids coated with Parlodion film, and stained with a saturated aqueous solution of uranyl acetate followed by lead citrate (22). A thin layer of carbon was evaporated onto the surface of the sections before viewing with a Philips-300 electron microscope. Pictures were taken at magnifications ranging from 10,000 to 40,600 diameters. The dimensions of structures were measured on enlarged micrographs or directly on negatives, using a Nikon Shadowgraph

(Nikon Inc., Instrument Div., Sub. of Ehrenreich Photooptical Industries, Inc., Garden City, N.Y.).

Preparation of Cell-Surface Membranes by Homogenization

For each preparation, the urinary bladders of three rabbits were dissected out and placed on ice. All subsequent steps were carried out at 0°–4°C. The bladders were slit open and tacked onto a dissecting board, with the lumenal surface exposed. Transitional epithelial cells were gently scraped off with a dull scalpel. Care was taken not to include underlying connective tissue. The scrapings were placed into ~2 vol of 0.25 M sucrose-TM[1] (0.005 M Tris-HCL and 0.002 M $MgSO_4$ at pH 7.4) and homogenized with 25 strokes in a 10 ml Potter-Elvehjem glass-Teflon grinder driven at 2500 rpm.

The homogenate was diluted to 10 ml with 0.25 M sucrose-TM and centrifuged at 2000 *g* for 15 min in a Sorvall HB-4 swinging bucket rotor to form a pellet, which was shown by electron microscopy to contain mainly cell-surface membranes, nuclei, and unbroken cells. This pellet was resuspended in 0.5 ml of 1.3 M sucrose-TM and homogenized with five strokes of the grinder.

The homogenate was layered over a 4 ml continuous sucrose-TM gradient extending from 1.3 M to 1.8 M and then centrifuged at 150,000 *g* for 30 min in a Spinco 50L swinging bucket rotor. The cell-surface membranes and their contaminants accumulated in a band near the top of the gradient, whereas the nuclei and cell debris settled in a pellet at the bottom of the tube.

The band enriched with cell-surface membranes was removed with a pipette, resuspended in TM or distilled water, and washed three times by centrifugation at 2000 *g* for 15 min in the HB-4 rotor. Electron microscopy revealed that the final pellet, although enriched with cell-surface membranes from epithelial cells, contained numerous contaminants, most notably nuclei.

Pellets enriched with cell-surface membranes were resuspended in 0.5 ml of 0.25 M sucrose-TM and diluted to 4.5 ml with 2% glutaraldehyde in phosphate buffer (pH 7.4). After 1 hr of fixation, the membranes were sedimented by centrifugation at 4000 *g* for 15 min in the Sorvall HB-4 rotor and processed thereafter as pellets in 15-ml glass centrifuge tubes. After postfixation in osmium tetroxide and alcoholic dehydration, the pellets were gently broken into quarters, placed in propylene oxide, and finally embedded in Epon (17). Blocks were oriented so that the plane of thin sections included the entire thickness of the pellet.

A procedure for isolating lumenal plasma membranes with 0.01 M sodium thioglycolate (pH 7.4) is described in the following paper (4), and was used for the preparation seen in Fig. 15.

Freeze-Etching

Both prefixed and unfixed tissues were processed for freeze-etching. Bladder tissues, prefixed for 15 min in 6% glutaraldehyde in 0.1 M cacodylate buffer (pH 7.6) or in Karnovsky's (13) fixative, were infiltrated with 30% glycerol over a 2 hr period. Unfixed bladder tissues were rinsed with 0.1 M phosphate buffer (pH 7.4) before being either infiltrated with 25% glycerol over a 1 hr period or washed with dilute TM buffer. Glycerol-infiltrated tissues were allowed to stand at room temperature for 30 min before they were cut into small cubes, placed on gold grids with a microspatula, and rapidly frozen in Freon 12 (−150°C). Tissues washed with dilute TM buffer were processed without further delay. Freeze-etch replicas were made on a Balzers BA360M freeze-etch machine (Balzers AG, Balzers, Liechtenstein) according to the method of Moor and Mühlethaler (18). The cleaved specimen surfaces were etched at −100°C for 5 sec to 3 min. Pellets of isolated cell-surface membranes suspended in water or dilute TM buffer were processed in a similar manner, except that no glycerol was added to specimens used for deep-etching experiments.

Surface area measurements of plaque and interplaque regions were made by cutting out these regions on enlarged micrographs and then weighing the two components. The area covered by each component is directly proportional to its weight.

Optical transforms of electron micrographs were prepared with a diffractometer built according to the design of Klug and DeRosier (15).

The encircled arrows in the lower right-hand corner of freeze-etch micrographs indicate the direction of shadowing.

Negative Staining

Sodium phosphotungstate (pH 7.2) was used for negative staining of plasma membrane fractions in a manner similar to that described by Benedetti and Emmelot (1).

RESULTS

Lumenal Membrane and Apical Cytoplasm in Cross-Sectional Views

Cells in the superficial layer of the epithelium bordering the lumen of the rabbit urinary bladder

[1] *Abbreviations used are:* rpm, revolutions per minute; TM, 0.005 M Tris-HCl and 0.002 M $MgSO_4$ (pH 7.4).

exhibit the same morphological features as those reported for mice (19) and rats (7). In both freeze-etched and sectioned specimens, the plasma membrane facing the lumen appears scalloped due to the presence of concave plaques alternating with crests formed by interplaque membrane material (Figs. 1–4). In the cortical cytoplasm a dense feltwork of filaments results in a prominent ecotplasmic layer that varies from one to a few microns in thickness. Within this layer and throughout the cytoplasm are many characteristic vesicles having the form of biconvex discs and a fusiform profile when sectioned or fractured at a normal angle.

In thin sections the plaques on the lumenal surface, as well as the similar portions of membrane limiting the discoidal vesicles, possess an unusually thick (~120 A) unit membrane (Figs. 3, 4). The lumenal leaflet is in both cases about twice as thick as the cytoplasmic one and occasionally exhibits a periodic structure (Fig. 3) with a repeating distance of ~130 A. Images of transversely fractured plaques in freeze-etch replicas also consist of two parallel leaflets of unequal thickness (Fig. 5). The over-all thickness of such cross-fractured membranes is also ~120 A, with the cytoplasmic leaflet measuring ~40 A across and the lumenal one measuring ~80 A. Thus, the bilayered structure of transversely fractured membranes observed in freeze-etched preparations corresponds to the images of asymmetric unit membranes seen in conventionally sectioned material (compare Figs. 3 and 4 to 5).

When viewed on edge in freeze-etch preparations, the lumenal or outer leaflet appears as a ridge composed of rows of granules separated by short lengths of smooth, unstructured material (Fig. 6). The distribution of granules, therefore, corresponds to the thick, outer leaflet of the plaques, the one exhibiting periodic structure in sectioned material, whereas the smooth regions correspond to the crests formed by interplaque membrane (compare Figs. 3 and 6).

Membrane Faces Exposed by Freeze-Cleaving

The structures responsible for this alternating sequence of rows of granules and smooth regions can be recognized in images of extensive areas of membrane faces (*PB* faces, Figs. 7, 8, 9, and 10) exposed by freeze-cleaving. The PB faces represent the split, inner faces of the outer or lumenal leaflets. The ridge (*R*, Figs. 7 and 8) of membrane material separating the face (PB) from the adjacent cytoplasm is ~40 A thick and thus corresponds to the dimensions of the cytoplasmic layer of transversely fractured membranes (see Fig. 5). Topographically, PB faces are characterized by polygonal plaques of particles forming hexagonal arrays (Figs. 7, 8, 9, and 10), with no apparent correlation between the orientation of the hexagonal arrangement in adjacent plaques. The plaques vary in shape and range from 0.1 to 0.6 μm in diameter. They are separated over intervals of 0.02 -0.3 μm by smooth interplaque regions, which exhibit no geometrical patterns. The material of the interplaque regions appears continuous with and identical to the material located between the particles of the plaques (Figs. 9, 10, 11, and 12). Approximately 73% of the surface area of PB faces is taken up by the plaques and ~27% by the interplaque regions. Particulate arrays identical to those on PB faces of the plasma membrane are also observed on the convex faces of discoidal vesicles (Fig. 2), which are oriented toward the cytoplasm, as is characteristic of PB faces.

The center-to-center spacing of the particles in the hexagonal arrays on PB faces is ~160 A. At higher magnification, the appearance of some of

FIGURE 1 Freeze-etch replica of the apical portion of the transitional epithelial cell of rabbit urinary bladder. The scalloped plasma membrane (*PM*) bordering the lumen (*L*) of the bladder is marked by deep infoldings (large arrows), which indicate the contracted state of the bladder at the time it was frozen. The cell cortex just beneath this surface is reinforced by a thick feltwork of cytoplasmic filaments (*F*). Within this layer and throughout the cytoplasm are many discoidal vesicles characterized by their fusiform profiles (*FV*). Some of the fusiform vesicles, as well as vesicles which appear more dilated (*DV*), have patches of hexagonally arranged particles which are barely discernible at this mganification. Mitochondria (*M*) and other unidentified vesicular orgaenelles are seen. The membranes in the upper left corner of the micrograph (double arrow), exhibit patches of hexagonally patterned material and may belong to a Golgi complex. × 25,000.

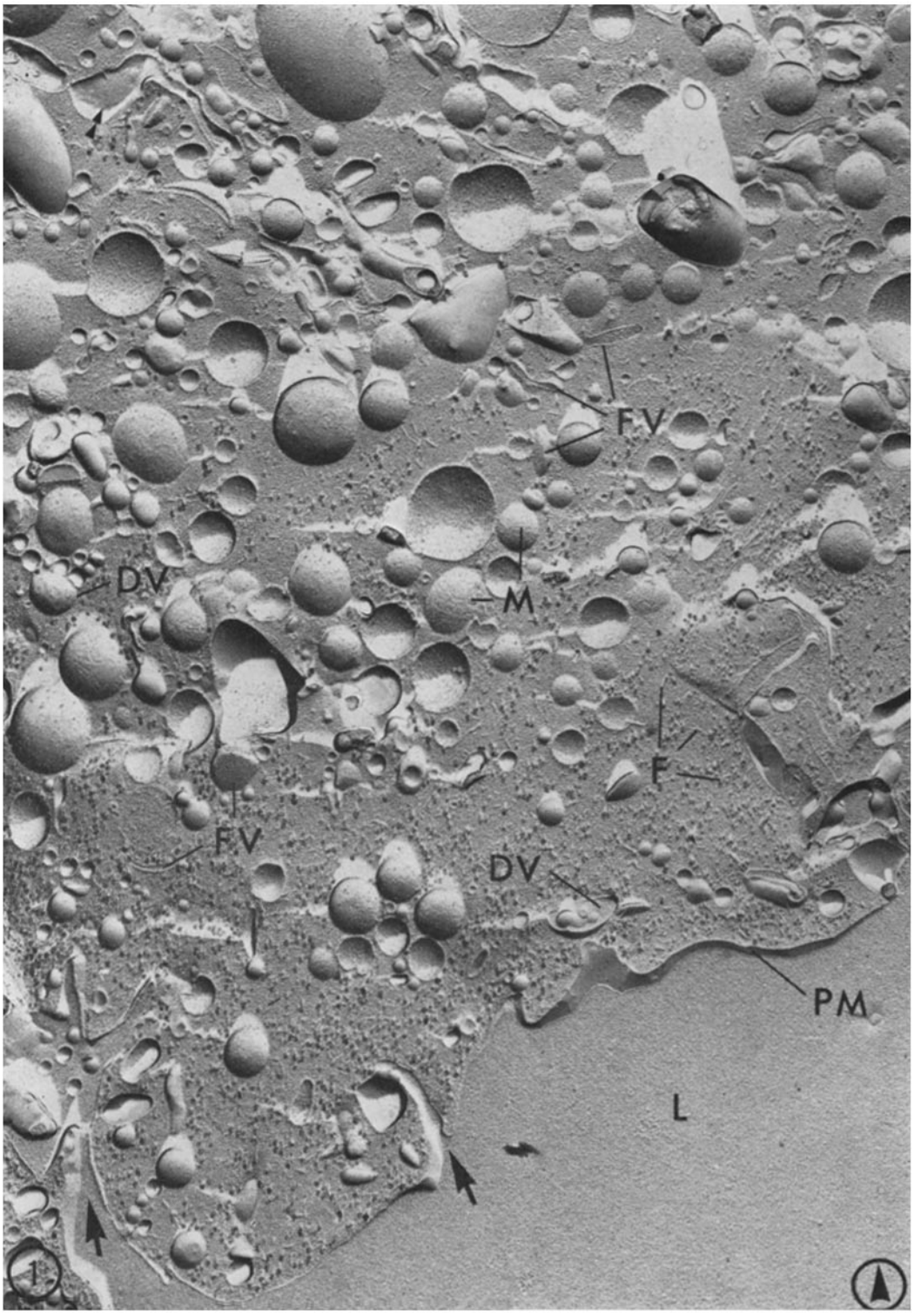
FV
DV
M
F
FV
DV
PM
L
1

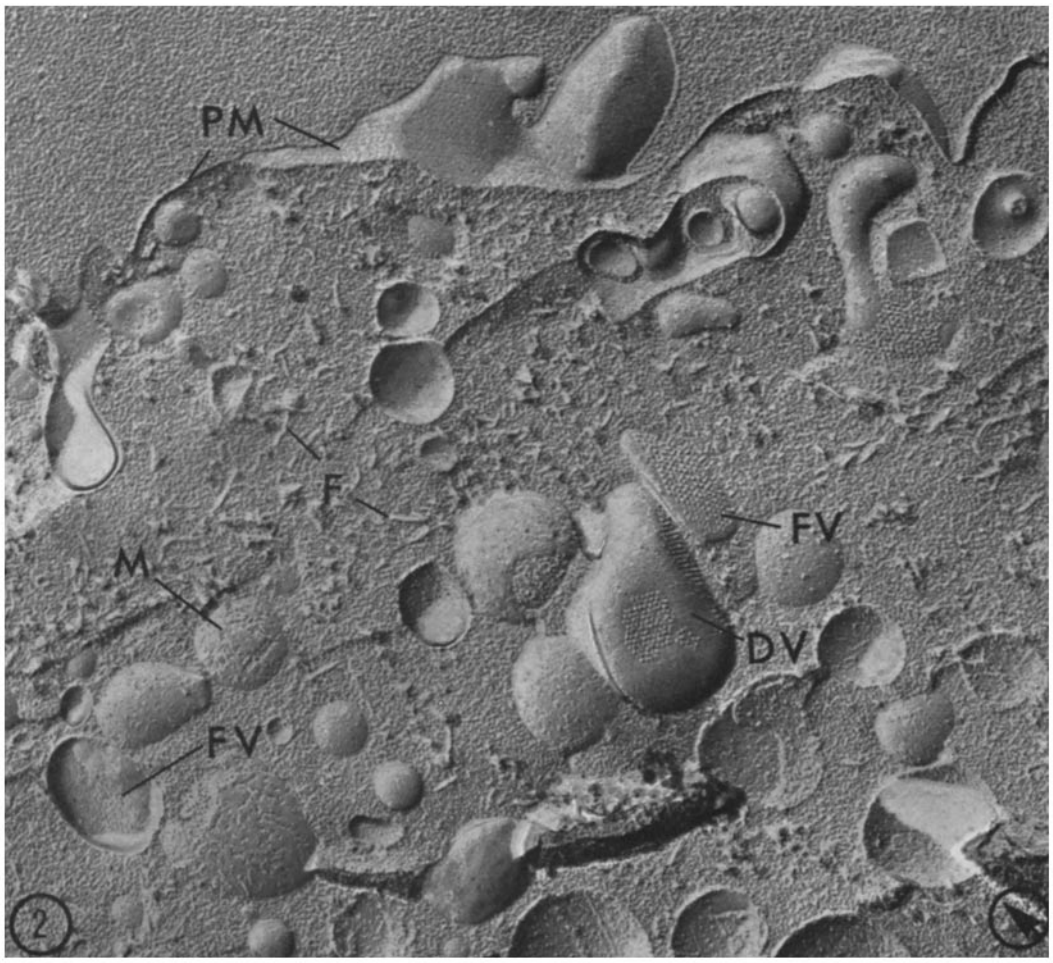

FIGURE 2 Higher magnification of a freeze-etched preparation of the lumenal border of a cell in a contracted bladder. The plasma membrane (*PM*) has an angular appearance with facets of the exposed face exhibiting a barely visible hexagonal pattern of fine indentations. A similar pattern of holes can be observed on the face of a fusiform vesicle (*FV*) in the lower left corner, while other fusiform (*FV*, center right) and dilated vesicles (*DV*) reveal membrane faces with prominent hexagonal arrays of particles. A few mitochondria (*M*) and numerous filaments (*F*) are the other main components in the apical cytoplasm of these cells. × 46,000.

these particles suggests that they may possess a substructure (encircled areas, Fig. 10). This notion of a substructure also is supported by the observation that the periodicity of the hexagonal arrays sometimes varies, undergoing a transition from large particles with a center-to-center spacing of ~160 A to smaller globules with a center-to-center spacing of ~50 A (Fig. 10). Analysis of the transition zone between the coarse and the fine pattern suggests that the finer one probably results from subunits within the larger particles. The demonstration of these finer patterns on PB faces seems to depend on the angle of attack of the cleaving forces; regions with fine patterns occur only in somewhat "protected" membrane areas on fairly steep sides of depressions facing away from the cutting edge of the microtome knife. For example, in Fig. 10, the cutting direction was approximately from the left to the right of the micrograph.

In addition to the PB faces, which represent split, inner faces of lumenal leaflets, freeze-cleaving

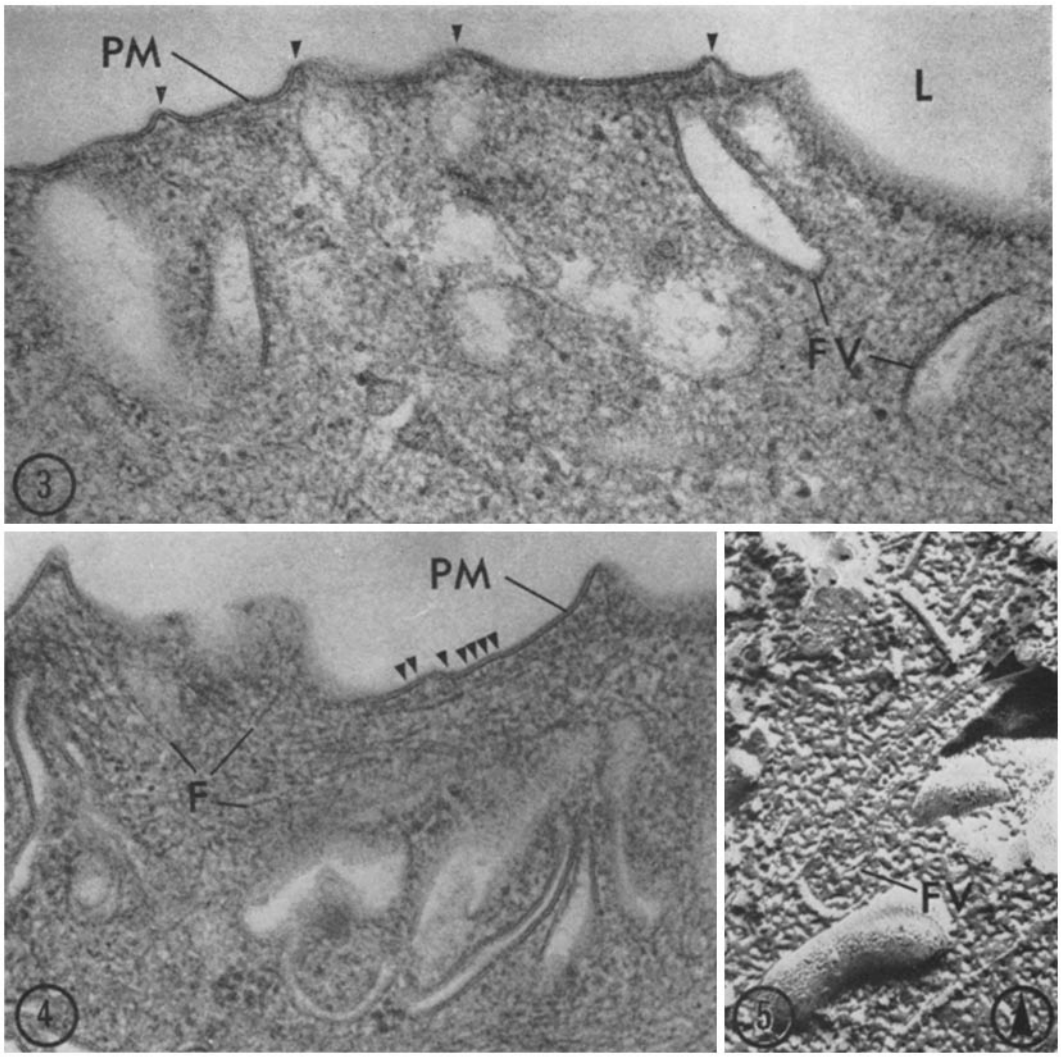

FIGURE 3 Thin section through the superficial region of a cell showing the lumen (*L*), the scalloped profile of the plasma membrane (*PM*), and a few discoidal vesicles which appear fusiform (*FV*) when sectioned transversely. The arrowheads point to crests of interplaque membrane material. Within the concave plaque regions the outer leaflet of the cell membrane is slightly thicker than the inner and in some areas appears to consist of subunits spaced at ~130 A. × 65,000.

FIGURE 4 A thin section oriented like that in Fig. 3 but selected to illustrate filaments in the cortical cytoplasm underlying the specialized plasma membrane (*PM*). Most of the filaments (*F*) in the vicinity of the cell surface run roughly parallel to the cell membrane. In some areas the staining densities suggest that the filaments might be attached to the inner surface of the membrane through short filamentous cross-bridges (arrowheads). × 65,000.

FIGURE 5 A transversely fractured fusiform vesicle (*FV*) in a freeze-etched cell. The vesicular membrane consists of a thinner cytoplasmic leaflet (small arrowhead) which is ~40 A wide, and a thicker lumenal leaflet (large arrowhead) which is ~80 A wide. × 126,000.

also exposes split, inner faces of cytoplasmic leaflets that are oriented towards the lumen (Figs. 2, 11, and 12). These faces, referred to as PA faces, are covered by polygonal areas of hexagonally arrayed holes with a center-to-center spacing of ~160 A. A ridge, corresponding to the particulate lumenal leaflet, can be observed separating PA faces from the lumen (Figs. 11 and 12). The rows of hexagonally arranged holes, when at the junction of a PA face with the transversely fractured outer leaflet, correspond one-to-one with the particles on the outer leaflet (small arrowheads, Fig. 12). Where the PA face is apposed to the particle-free interplaque region of the outer membrane leaflet, no such pattern of holes is visible. Thus, PA faces appear to be complementary molds into which the various elements from PB faces fit. Patterns of holes, identical to those on PA faces of plasma membranes, are also observed on split surfaces of discoidal vesicles, in which concave faces are oriented towards the intravesicular space (*FV*, at left, Fig. 2).

Unlike the striking particulate patterns of PB faces, which remain visible even after prolonged etching, the clarity of the shallow holes on PA faces is more difficult to preserve and visualize. Prolonged etching destroys the pattern of holes (Fig. 13), and even when preserved they are distinct only in areas shadowed at relatively low angles.

External Surface of Lumenal Membrane

Freeze-cleaving followed by a short of no etching period reveals only split, inner membrane faces (PA and PB faces), which result from fracturing the membranes along the plane between the thicker and thinner leaflet. One must etch specimens a few minutes (deep-etching) in order to expose larger areas of the true lumenal surface and the true cytoplasmic surface of the plasma membrane. However, the presence of cytoplasmic matrix adjacent to the cytoplasmic surface and of some unidentified contaminating material on the lumenal surface made complete sublimation of frozen water from these faces difficult in whole tissue specimens. Therefore, we isolated and washed plasma membranes in either distilled water or dilute TM buffer before freeze-etching. In such specimens, the lumenal and cytoplasmic surfaces can be exposed with greater clarity by the deep-etching. Membranes washed and frozen in dilute TM buffer were generally better preserved than those washed and frozen in distilled water.

Figs. 13 and 14 are representative views of the lumenal surfaces of isolated plasma membranes exposed by prolonged etching. On these surfaces (PO faces), plaques of various sizes are recognized by their hexagonal surface patterns and by their protruding particles. The smooth surfaces of the interplaque regions lack any repeating elements and are separated from the plaques by a step. The difference in height of plaques and interplaque regions is consistent with the greater thickness of the oute membrane leaflet in the plaque regions seen in transversely fractured membranes (see Figs. 5 and 12). At high magnifications, the particles protruding from the lumenal surfaces of

FIGURE 6 Edge-on view of the lumenal leaflet of the plasma membrane of a freeze-cleaved epithelial cell lining the lumen of the bladder. The transversely fractured layer consists alternately of rows of granules and segments of smooth, unstructured material. The arrows point to the particle-free interplaque membrane regions. × 90,000.

FIGURE 7 Freeze-etched cell in which some of the cortical cytoplasm (*C*) has been removed by the cleavage process to expose the split inner face (*PB*) of the lumenal leaflet of the specialized plasma membrane. This membrane face has at its base a barely visible ridge (*R*), which represents the cytoplasmic membrane leaflet in cross-section. The mosaic appearance is due to the presence of hexagonally patterned plaques of different sizes and shapes on an otherwise smooth background. The arrow points to a piece of membrane, possibly part of a fusiform vesicle, which is attached through a narrow neck to the undifferentiated interplaque region of the plasma membrane. Bladder lumen (*L*). × 50,000.

FIGURE 8 Folded apical plasma membrane of a cell taken from a collapsed bladder. This freeze-etch micrograph of the same type of split membrane face (*PB*) as shown in Fig. 7 illustrates that the sharp folds in the membrane coincide with smooth interplaque regions. The cross-sectioned cytoplasmic membrane leaflet can be recognized in some areas as a ridge (*R*) at the base of the *PB* face. Numerous filaments lie in the cytoplasm (*C*). Bladder lumen (*L*). × 40,000.

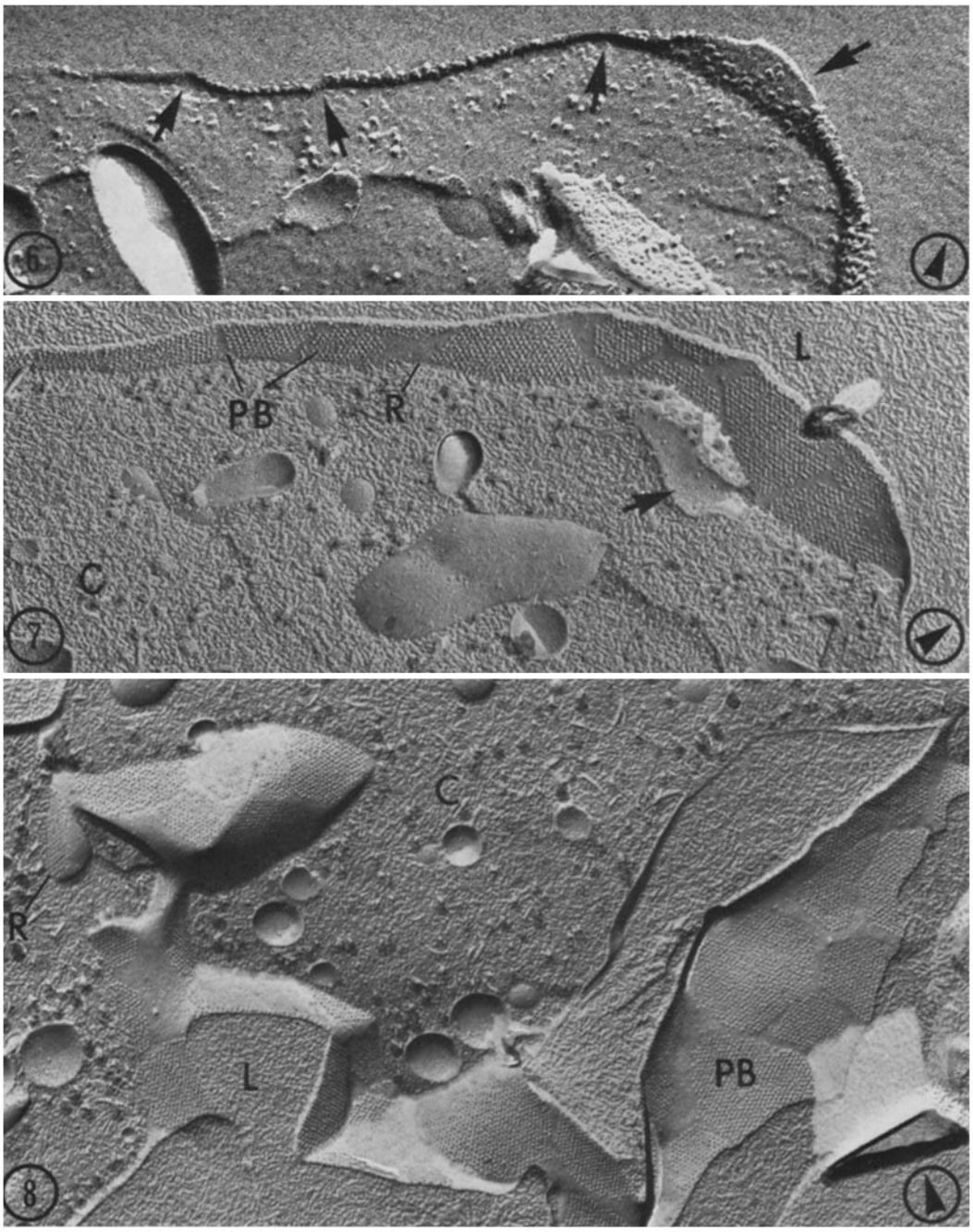
6
PB
R
L
C
7
R
C
L
PB
8

plaques frequently exhibit a central depression, and at very low shadowing angles each of these ringlike structures can occasionally be resolved further into six subunits forming a hexagon (Fig. 14).

To confirm that the subunit structure revealed by freeze-etching was real and did not arise from aggregates of shadowing materials coincidentally arranged in the form of hexagons, optical transforms of images of PO surfaces of plaques similar to the one shown in Fig. 14 were prepared (Fig. 15 A). These patterns were then punched into aluminum foil masks and together with the original negative a filtered image of the hexagon was produced (Fig. 15 B). The resulting image seems to confirm the subunit structure of the hexagons, which also can be discerned in preparations of isolated membranes negatively stained with phosphotungstic acid (Fig. 16). In such negatively stained specimens interplaque regions are difficult to visualize. However, both methods show the center-to-center spacing of the hexagons to be about 160 A and the center-to-center distance between the subunits to be about 50 A.

Cytoplasmic Surface of Lumenal Membrane

Representative views of cytoplasmic surfaces of isolated plasma membranes revealed after deep-etching are seen in Figs. 17 and 18. These surfaces, referred to as PI faces, show no surface pattern except for the barely discernible presence of filamentous elements. Thus, PI faces, unlike PO, PA, and PB faces, have no hexagonal arrays of particles or corresponding depressions. The small filamentous elements associated with the cytoplasmic surface of isolated membranes are more evident in sectioned preparations (Fig. 19). In such images, short filaments appear to cross-link numerous long cytoplasmic filaments to the inner leaflet of the membrane (Fig. 19 and insert). Many of the long cytoplasmic filaments run parallel to the membrane surface and seem to interconnect with a meshwork of similar filaments farther away from the surface. In some instances, long filaments are also seen to tie together separate plaque regions (Fig. 19). The architecture and interconnections of long cytoplasmic filaments with short membrane-associated filaments are more apparent in isolated membranes (Fig. 19) than in intact cells (Figs. 3 and 4), probably due to the removal of electron-opaque cytoplasmic ground substance during the isolation procedure. In freeze-cleaved specimens short filamentous bridges occur at the base of PB faces, where they apparently attach to the tips of the particles making up the plaques (Figs. 20 and 21). The interplaque regions are devoid of short, bridging filaments.

Nature of the Interplaque Membrane Region

In both sectioned (Figs. 3, 4, and 19) and freeze-etched preparations (Figs. 1, 2, 8, 11, and 13) the lumenal membranes are bent in the particle-free interplaque regions. These bends are sharpest in

FIGURE 9 Large area of a split PB face demonstrating that the polygonal plaques vary considerably in form and in size. The width of the smooth, undifferentiated interplaque regions is also subject to variation. Round holes can be seen in some areas of the interplaque regions (arrows). These may represent necks of attached discoidal vesicles broken off in the process of freeze-cleaving. The optical transform shown in the upper left corner was made from the plaque marked by a star and confirms that the large particles are indeed arranged in a hexagonal array with a repeating distance of ~160 A. Bladder lumen (*L*). × 46,000.

FIGURE 10 A higher magnification of the area of the PB face marked by the rectangle in Fig. 9. The plaque indicated by the arrow exhibits a sudden transformation of the dominant hexagonal array of large particles into a finer, less clearly defined one of smaller particles. These finer patterns are observed only in plaques located in slopes facing in the cutting direction of the knife edge. They are interpreted as arising from and being manifestations of the subunits of the larger particles. The appearance of some of the larger particles. (encircled areas) and of the optical transform (upper left corner) prepared from the plaque area marked by a star also suggests the presence of subunits within the larger particles. The smooth surface of the interplaque regions appears continuous and level with the surface of the material located between the particles. The noticeable deviation from the hexagonal symmetry of the patterns is due to the fact that the membrane area is seen at an angle smaller than 90°. × 126,000.

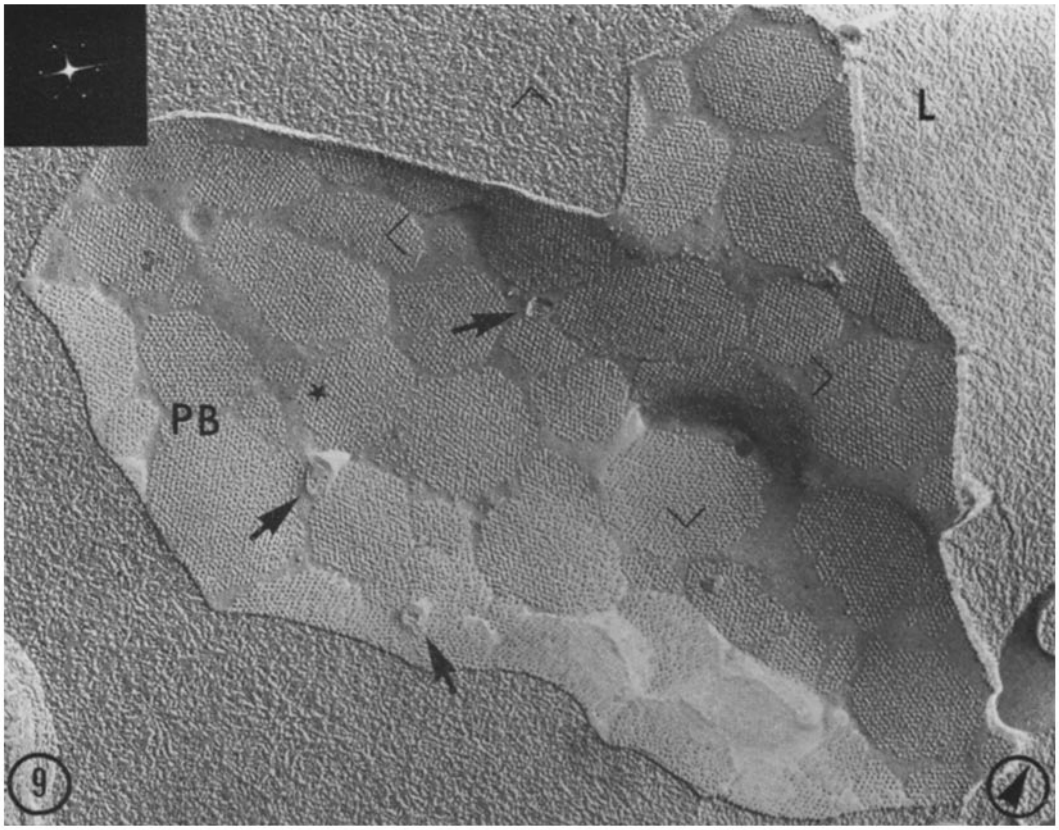
L
PB
9

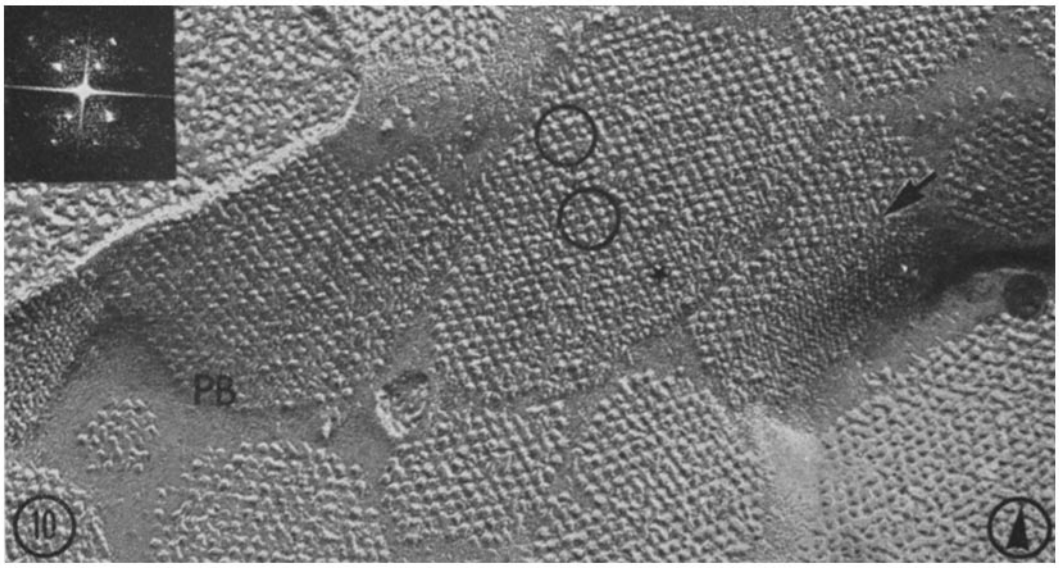
PB
10

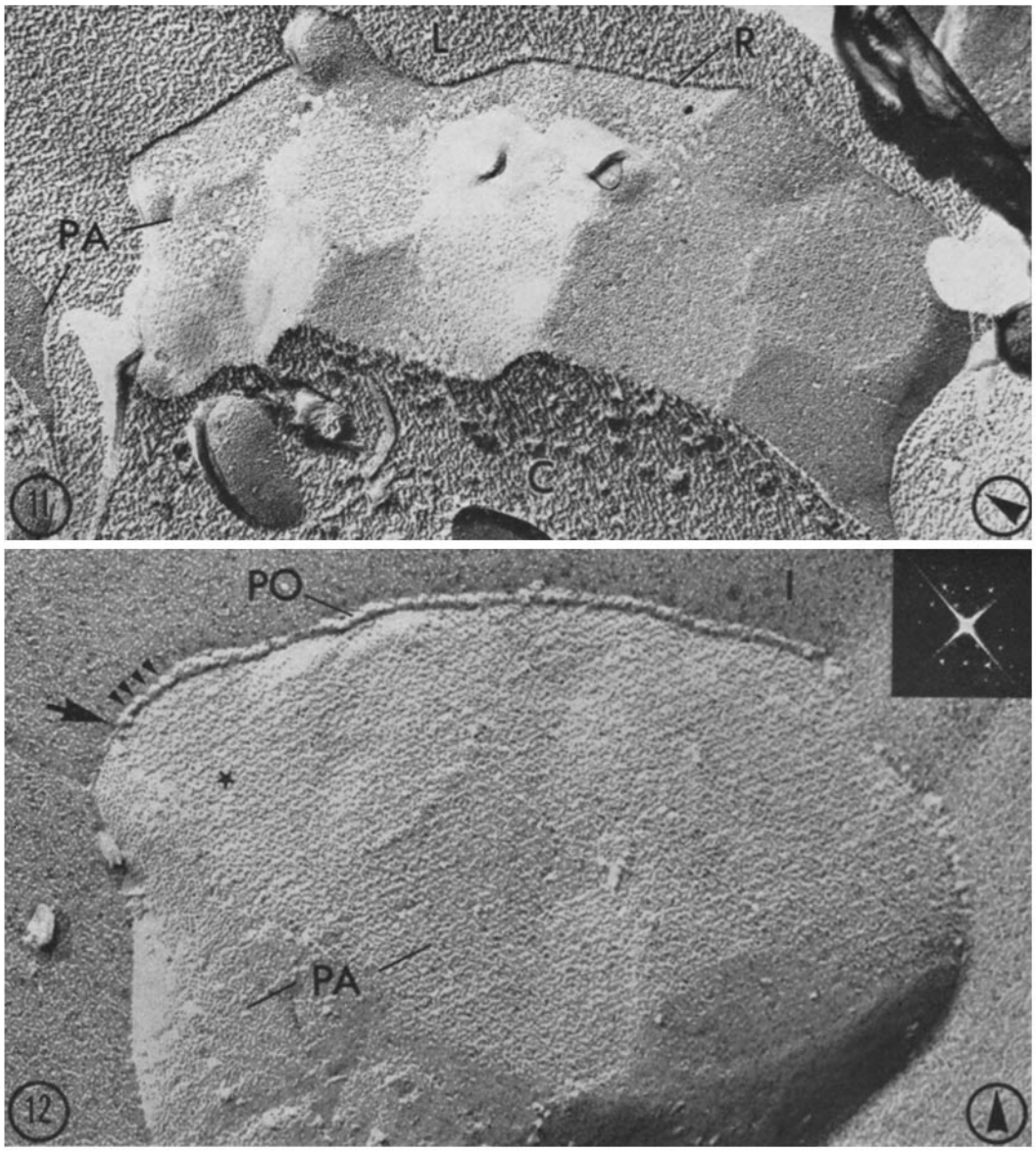

FIGURE 11 Micrograph of the split inner face (*PA*) of a cytoplasmic membrane leaflet revealed by the cleaving process. PA faces are oriented towards the lumen (*L*) and are complementary to PB faces. The holes forming the hexagonal patterns within the plaque regions of such PA faces have center-to-center spacings of ~160 A, the same as the particles of the arrays on the PB faces. Notice the continuity of the material making up the membrane matrix both in plaque and in interplaque regions. The pronounced ridge (*R*) at the upper edge of the face (*PA*) represents a cross-sectional view of the lumenal membrane leaflet. Cytoplasm (*C*). × 90,000.

FIGURE 12 An area of plasma membrane isolated from transitional epithelium, washed and frozen in distilled water, freeze-cleaved, and etched for 5 sec at −100°C before replication. The split inner membrane face (*PA*) exhibits a fine hexagonal array of holes coinciding with a plaque region. It is characteristic that the individual holes do not show up very clearly. This lack of clarity seems to be caused by the presence of a substructure within the holes, which may be complementary to the substructure of the particles illustrated in Fig. 10. Further support for the notion of a substructure within the holes comes from the appearance of the optical transform (upper right corner) prepared from the starred membrane area. No pattern is apparent in the interplaque region (lower left). Notice how the cross-sectioned outer membrane leaflet at upper edge of the patterned PA face area is composed of particles (small arrowheads) which seem to extend to the membrane surface (*PO*) and which make the leaflet approximately twice as thick as in smooth areas where it abuts on interplaque regions. This difference in thickness of the outer membrane leaflet between patterned plaque and smooth interplaque regions gives rise to steps on varying levels of elevation on the lumenal membrane surface (see Figs. 13 and 14). The large arrow indicates a point of transition between plaque and interplaque regions of the outer leaflet. Ice (*I*). × 123,000.

the cells of contracted bladders, which contain deep infoldings of the plasmalemma (Fig. 8). The plaques, on the other hand, are never bent at sharp angles; rather, they appear more rigid, usually maintaining a slight curvature which produces a concave surface facing the lumen.

In some images, especially of unfixed specimens, membranous diverticula are occasionally found attached to the cytoplasmic side of the lumenal plasma membrane (Fig. 7). These elements are continuous through relatively narrow necks to the interplaque regions, not to the plaques themselves. The general form and size of these structures is consistent with their being discoidal vesicles pinching off from and/or fusing with the plasma membrane. This phenomenon is also suggested by the presence of round holes in interplaque areas of cleaved membranes (Fig. 9). These holes are oriented toward the cytoplasm and might represent the necks of attached discoidal vesicles, broken off in the process of freeze-cleaving.

DISCUSSION

The data presented in this report indicate that the specialized lumenal membranes of transitional epithelial cells are a mosaic of plaques. Each plaque is composed of hexagonally arrayed particles and linked to adjacent plaques by particle-free interplaque regions. Porter et al. (21) have already postulated this structure from their study of sectional material. On the other hand, our findings are at variance with those of Hicks and Ketterer (11) who report that the particulate arrays are continuous over the whole membrane surface. However, their observations were confined to negatively stained specimens, in which we find interplaque regions difficult to discern (see Fig. 16).

The Permeability Barrier of the Transitional Epithelium

Transitional epithelium has been reported to maintain a permeability barrier to the exchange of water and salts between the blood and urine (6, 12). Hicks (7, 8) has suggested that this barrier is located in the specialized lumenal plasma membrane and has attributed its impermeability to the presence of keratin. It was logical to assume that the thickened lumenal membrane, with its particles, constituted the barrier—especially if the particles covered the entire lumenal surface (11). However, as we have shown, particles are absent from the thinner membrane segments of the interplaque regions, which appear to make up as much as 27% of the lumenal surface area. Therefore, it seems unlikely that the particles entirely could account for the permeability properties of these membranes. Instead, it seems more likely that other components, present in both the plaque and interplaque regions, would be responsible. The experiments reported in the following paper (4) present evidence that lipids and/or other hydrophobically associated molecules probably are important in this regard.

Fine Structure of the Lumenal Membrane and its Relationship to Underlying Cytoplasm

In freeze-etched replicas, four easily identifiable membrane faces are observed, as summarized in the model presented in Fig. 22. The interplaque regions are smooth on all the faces; but this was most strikingly evident on the split, inner faces (PB) of lumenal leaflets where the interplaque regions contrasted sharply with the particles of the plaques (Figs. 7, 8, 9, and 10). In such micrographs it is also seen that the smooth surface of the interplaque material is continuous with the material filling the spaces between the particles of the plaques. Such smooth faces have been reported to be typical of membranes with a high lipid content, in which lipids are arranged in a bilayer (2, 3, 5). Experiments reported in the following paper (4) support this idea.

The plaques are irregularly shaped polygons of various sizes (Figs. 8, 9, and 13). All of their particles remain attached to the outer leaflet during the cleaving process (Figs. 6, 7, 8, 9, and 10). In all other plasma membrane systems studied thus far, the asymmetry of the fracture plane has not only been less pronounced, but usually reversed, with the majority of the particles adhering to the inner plasma membrane leaflet (3). This exceptional behavior of the lumenal plasma membrane could be explained by assuming that the particles of the hexagonal arrays are linked together in the lumenal leaflet. Such cross-linking between the particles and/or their subunits also could account for the constant curvature of the apparently rigid plaques.

As demonstrated in the results and presented in diagrammatical form in Fig. 22, the particles protruding from the split, inner PB face (Figs. 7, 8, 9, and 10) appear to be extensions of those jutting from the true lumenal surface (*PO* face;

Figs. 13, 14, and 16) and seem to fit into complementary holes in the split, inner PA face (Figs. 11 and 12). Since no hexagonal patterns are visible on the PI faces (Figs. 18 and 19), it seems unlikely that the particles extend beyond the cytoplasmic membrane surface. Nevertheless, as the height of the particles on PB faces is similar to the thickness of the cytoplasmic leaflet (~40 A), it is not unrealistic to suggest that the particles bridge most of the thickness of the membrane when they are *in situ*.

Our data are consistent with previously reported observations on negatively stained lumenal membranes isolated from rat and mouse urinary bladders (10, 11, 24), which demonstrated hexamers with a center-to-center spacing of ~160 A. A correlation of freeze-etched and negatively stained images (compare Figs. 14 and 16) indicates that the images of hexamers visible in negatively stained preparations most likely arise from negative stain surrounding the tips of subunits of the particles protruding from the lumenal surface. Vergara et al. (24) have reported that the hexamers are skewed about 19° with respect to the main rows of particles on membranes from mice, and a similar configuration has been found to exist on rat membranes (25). Our optical diffraction patterns (Figs. 15 A and B) of freeze-etch images of PO surfaces of plaques suggest the same substructure and the same 19° skewness of the hexamers in rabbit membranes. Therefore, it appears that the particulate arrangement is identical for rats, mice, and rabbits.

Recently, Warren and Hicks (25) have reported that each hexamer is, in fact, a dodecamer consisting of 12 subunits forming an outer and an inner ring, the whole arranged in a six-pointed stellate configuration. How the six points of the hexagonally arranged particles of our freeze-etched specimens are related to the 12 subunits of the dodecamer particles is not clear at present. It is possible that the six particles forming the outer ring of the proposed dodecamers protrude farther out of the membrane surface than those located in the inner ring. This would make the latter difficult to visualize both in negatively stained and in freeze-etch preparations. Supporting this hypothesis is the fact that the clear visualization of the inner ring of subunits in negatively stained preparations depends on the prior solubilization of some of the membrane lipids by detergents (Robertson, personal communication).

Although no particles seem to protrude through the cytoplasmic surface of the membrane (*PI* face; Figs. 17 and 18), small filamentous elements

FIGURE 13 Isolated plasma membrane, washed in TM solution, freeze-cleaved, and etched for 2 min before replication. The deep-etching has revealed the outer surface of the lumenal plasma membrane (*PO*), which in vivo would have been in contact with the urine in the bladder. The surface topography allows the distinction between hexagonally patterned plaque regions of varying size and interplaque regions (arrows). The particles of the plaque regions protrude beyond the surface level of the interplaque or hinge regions; thus they produce steps. The prolonged etching has obliterated the delicate details of the split inner membrane *PA* face. The pronounced ridge (*R*) marks the edge of the partly torn away lumenal membrane leaflet and separates the PA face from the PO surface. Etched ice surface (*I*). × 80,000.

FIGURE 14 Higher magnification of a plaque area of a PO surface. This membrane, unlike all the others presented in this paper, was subjected to 0.01 M thioglycolate solution for 5 min during the isolation procedure (4). The latter treatment plus a very low shadowing angle has allowed visualization of the six subunits that make up each particle (arrows). × 190,000.

FIGURE 15 A Optical transform of a plaque area of a PO surface similar to the one shown in Fig. 14.

FIGURE 15 B Reconstructed image of a plaque area of a PO surface obtained by filtering the pattern of Fig. 15 A so that only the rays forming the hexagonal pattern were admitted. The individual hexagons (arrowhead) show up clearly, thus indicating that the substructure of the particles demonstrated in Fig. 14 is real and does not represent a coincidental aggregation of shadowing materials.

FIGURE 16 Fragment of isolated plasma membrane which was washed in TM solution and negatively stained with phosphotungstic acid. The same hexagonal pattern can be discerned as in freeze-etch specimens. Interplaque regions cannot be recognized in this micrograph. × 160,000.

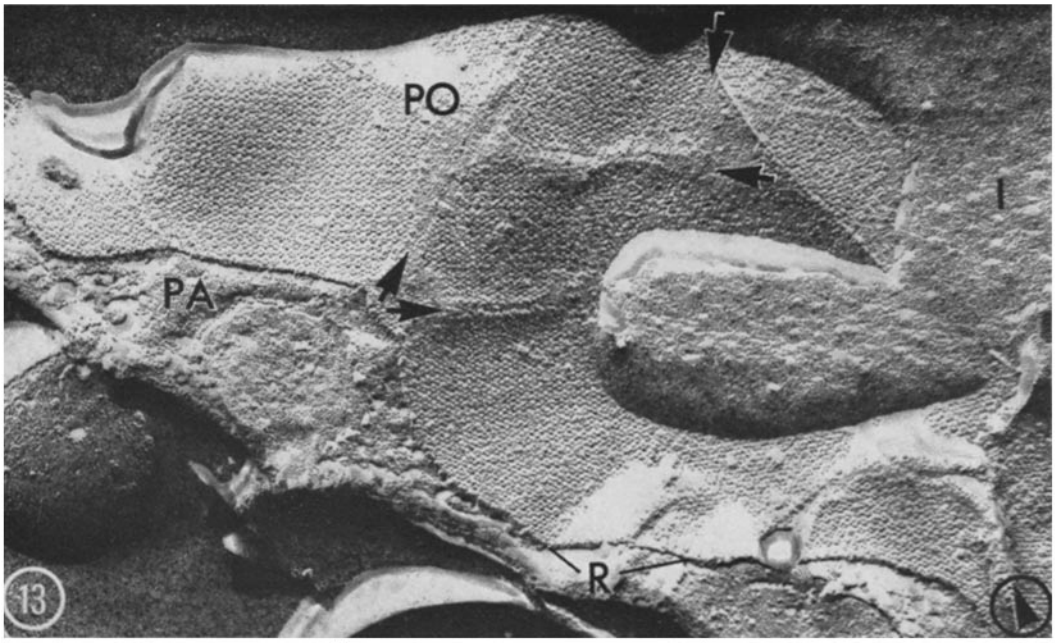
PO
I
PA
R
13

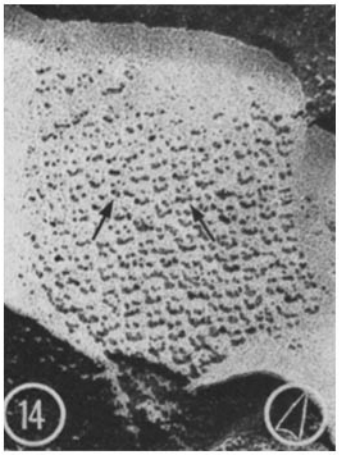
14

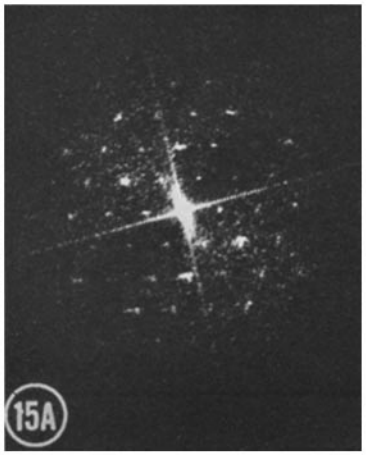
15A

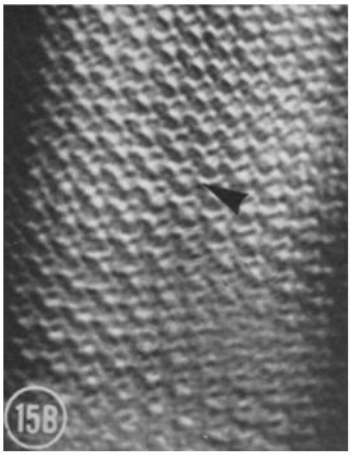
15B

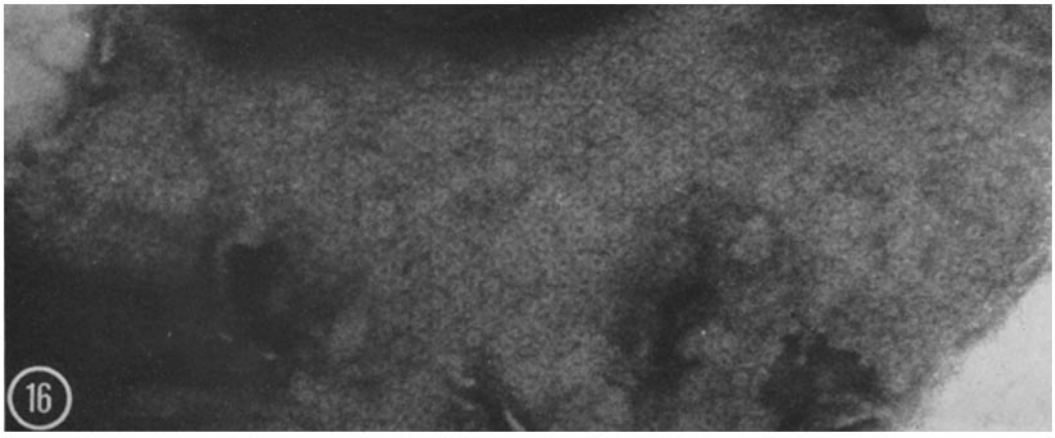
16

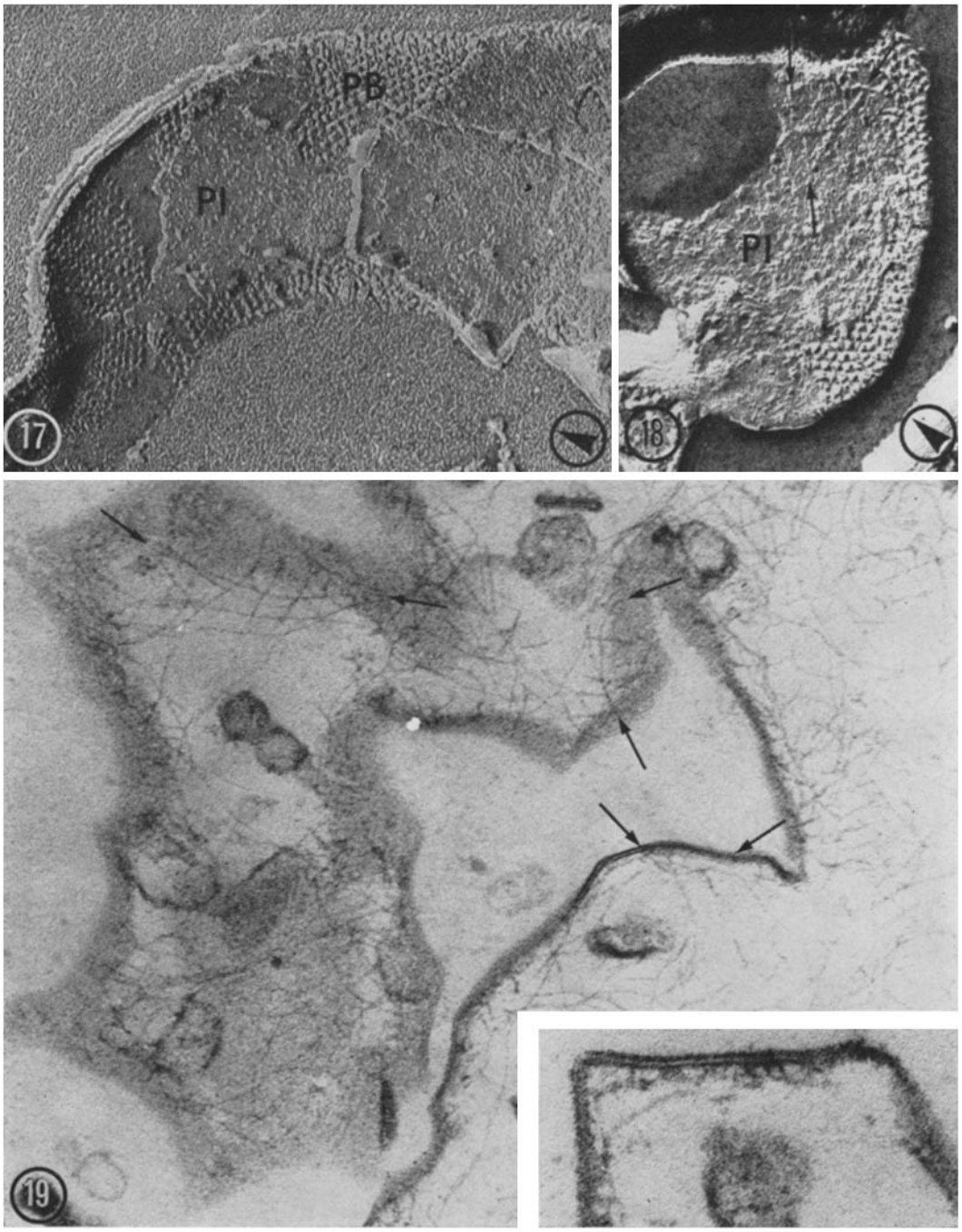

FIGURE 17 Freeze-etched fragment of an isolated plasma membrane washed in distilled water and etched for 15 sec before replication. Besides the particle-bearing split inner membrane face (*PB*), the cytoplasmic surface of the membrane (*PI*) is seen as a thin layer overlying the particulate arrays. × 75,000.

FIGURE 18 Micrograph of an isolated plasma membrane prepared like that in Fig. 17, except that it was etched for 60 sec. Outlines of what appear to be partly embedded filaments (arrows) can be detected on the stubbly cytoplasmic surface (*PI*) overlying the split inner membrane PB face that is identified by the arrays of particles. × 100,000.

FIGURE 19 A section through the lumenal portion of an isolated plasma membrane washed in distilled water before fixation. The most conspicuous feature of this micrograph is the association of numerous filaments with the cytoplasmic surface of the hexagonally patterned membrane, cut over most of its area at tangential and oblique angles. These filaments appear to cross-link different plaque regions (arrows). The attachment of the long filaments to the cytoplasmic surface of the membrane seems to be mediated by short cross-bridging filaments (*insert*). × 80,000; *insert:* × 125,000.

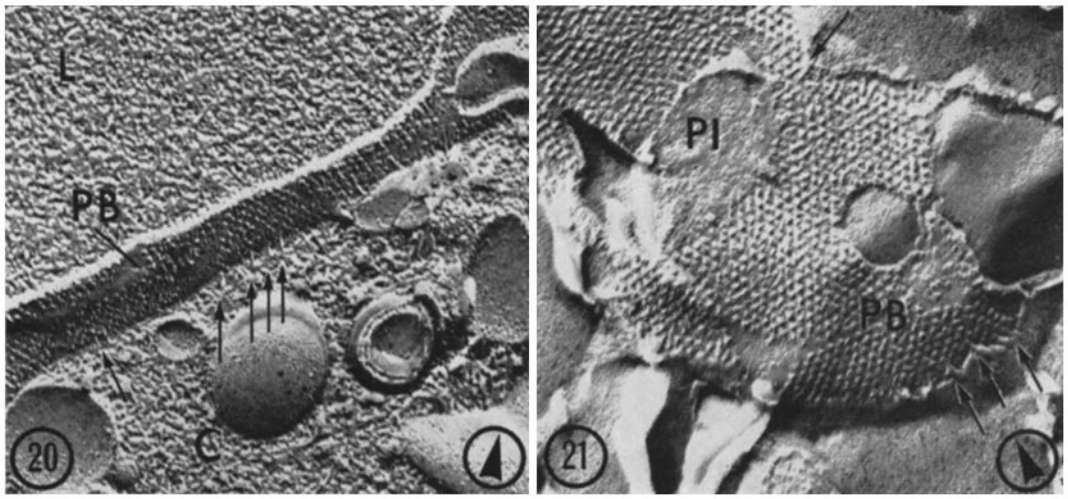

FIGURE 20 Apical region of a freeze-etched cell. Numerous short filaments (arrows) can be recognized leading from the cytoplasm (*C*) to the hexagonal arrays of particles belonging to the plaques of the split inner membrane *PB* face. Bladder lumen (*L*). × 76,000.

FIGURE 21 Freeze-etched fragment of an isolated plasma membrane which was washed in TM, freeze-cleaved, and etched for 90 sec before replication. A number of short filaments (arrows), similar to those illustrated in Fig. 20, can be observed around the edge of the split inner membrane *PB* face. These short filaments seem to be attached on one side to the plaque particles and on the other side seem to disappear into the material adhering to the cytoplasmic membrane surface which has been exposed by deep-etching. Cytoplasmic membrane surface (*PI*). × 80,000.

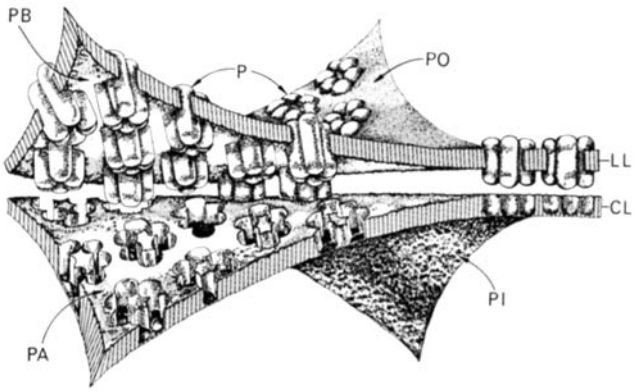

FIGURE 22 A diagram of our concept of the lumenal plasma membrane of urinary bladder epithelial cells, illustrating the relationship between the two split inner membrance faces (*PA* and *PB*) and the two external membrane surfaces (*PI* and *PO*). Cytoplasmic leaflet (*CL*); lumenal leaflet (*LL*); particles (*P*). The size and spacing of the membrane components are not precisely to scale.

are attached to it, and some images (Figs. 20 and 21) indicate that these filaments are anchored to the particles within the membrane. The attachments of long cytoplasmic filaments to the short filaments and the connections of the short filaments to the membrane (Figs. 4, 19, 20, and 21) are fairly stable, since these associations remain intact during the isolation procedure, despite homogenizations and washings of the membranes in distilled water or TM buffer. The proposed structural associations of these components are summarized in Fig. 23.

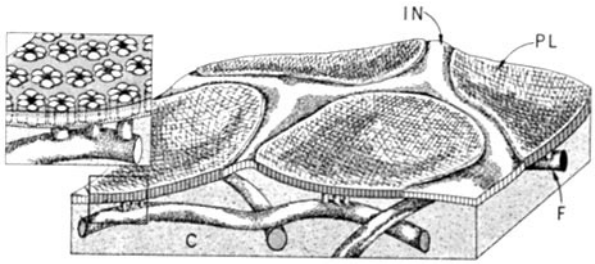

FIGURE 23 A diagrammatic view of the lumenal plasma membrane of urinary bladder epithelial cells. The outer lumenal surface of the hexagonally patterned, rigid plaques (*PL*) is elevated with respect to the surface of the flexible interplaque regions (*IN*) due to the protruding particles of the hexagonal arrays. The long cytoplasmic filaments (*F*) underlying the membrane seem to be attached to the hexagons of the plaques by means of short cross-bridging filaments (*insert*). Cytoplasm (*C*).

Functional Implications of the Described Structures

The surface area of the lumenal membranes is required to change greatly over short time intervals when the bladder distends and contracts. Porter et al. (20, 21) claim that some discoidal vesicles made up of opposing plaques pinch off from the cell surface during contraction, as indicated by their uptake of ferritin (20). Although this process may be important in the turnover of membrane material at the surface, it seems likely to us that the major adjustment in surface area that occurs upon each contraction of the bladder could be explained by a simple folding of the membrane. The images seen in the contracted bladder, that is folds of membrane extending into the cytoplasm (Figs. 1 and 8; cf. reference 15), are compatible with this interpreation.

High angles of curvature observed in the interplaque regions (Figs. 1 and 8) indicate that these areas have a capacity to bend to almost any angle and in either direction, as if they were hinges. Thus, the lumenal membrane can fold and unfold, somewhat like a concertina. However, in view of the apparent rigidity of the plaques and the irregularity of the distance between them, the actual folding would require translational movements of the plaques with a concomitant flow of interplaque material within the plane of the membrane as bending occurs in the interplane regions. The liquid crystalline properties of a lipid bilayer structure, such as the interplaque regions apparently have, would allow such rearrangements of the plaques during folding. Thus, the arrays of cross-linked plaque particles could be envisioned as floating in the bilayer matrix. In this regard, it is interesting that freeze-etch images of

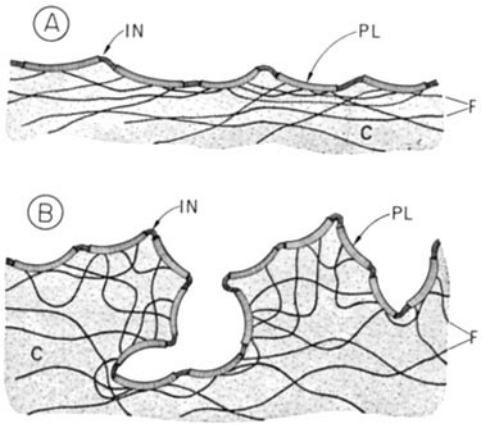

FIGURE 24 A simplified diagram of the lumenal region of urinary bladder epithelial cells in (A) the distended bladder and (B) the collapsed bladder. Cytoplasm (*C*); cytoplasmic filaments (*F*); interplaque regions (*IN*); plaques (*PL*).

split, inner PB faces (Fig. 9) are reminiscent of aerial photographs of pack ice illustrating large ice blocks floating on water.

If it is unlikely that the plaques constitute a permeability barrier or take part in reducing the lumenal surface during contraction of the bladder, then what is the function of these unique entities? Given the cross-linking of adjacent plaques by cytoplasmic filaments (Fig. 19), we suggest that the rigid plaques simply act as anchors for these filaments via the interconnections herein described (Fig. 23). Such a membrane-filament interaction could stabilize and strengthen the lumenal membrane, thereby preventing it from rupturing when the bladder is distended (Fig. 24 A). Furthermore, it is possible that their structural interlocking would promote an orderly infolding of the mem-

brane surface during contraction of the bladder (Fig. 24 B).

We are greatly indebted to Dr. Keith R. Porter for the use of his laboratory facilities and for his continued interest and critical discussions of this work. We thankfully acknowledge the help of Dr. J. Richard McIntosh in preparing the optical transforms. We are obliged to Henry V. Webber III and Dorothy Marion for their expert technical assistance.

This work was supported by Health Science Advancement Award Grant 5-S04-FR06084 to the University of Colorado, by National Institute of General Medical Science Grant 1 R01 GM18639 to the University of Colorado, by United States Public Health Service Grant GM 16880 to Harvard University, and by National Institutes of Health Fellowship GM37, 252 and Grant 1 R01 GM18332 to F. J. Chlapowski.

Received for publication 25 June 1971, and in revised form 17 December 1971.

REFERENCES

1. Benedetti, E. L., and P. Emmelot. 1965. Electron microscope observations on negatively stained plasma membrane isolated from rat liver. *J. Cell Biol.* **26**:299.
2. Branton, D. 1967. Fracture faces of frozen myelin. *Exp. Cell Res.* **45**:703.
3. Branton, D. 1969. Membrane structure. *Annu. Rev. Plant Physiol.* **20**:209.
4. Chlapowski, F. J., M. A. Bonneville, and L. A. Staehelin. 1972. Lumenal plasma membrane of the urinary bladder. II. Isolation and structure of membrane components. *J. Cell Biol.* **53**:92.
5. Deamer, D. W., R. Leonard, A. Tradieu, and D. Branton. 1970. Lamellar and hexagonal lipid phases visualized by freeze-etching. *Biochim. Biophys. Acta.* **219**:47.
6. Englund, S. E. 1956. Observations on the migration of some labeled substances between the urinary bladder and the blood in the rabbit. *Acta. Radiol. Suppl.* **135**:1.
7. Hicks, R. M. 1965. The fine structure of the transitional epithelium of rat ureter. *J. Cell Biol.* **26**:25.
8. Hicks, R. M. 1966. The permeability of rat transitional epithelium. Keratinization and the barrier to water. *J. Cell Biol.* **28**:21.
9. Hicks, R. M. 1966. The function of the Golgi complex in transitional epithelium. Synthesis of the thick cell membrane. *J. Cell Biol.* **30**:623.
10. Hicks, R. M., and B. Ketterer. 1969. Hexagonal lattice of subunits in the thick lumenal membrane of the rat urinary bladder. *Nature (London).* **224**:1304.
11. Hicks, R. M., and B. Ketterer. 1970. Isolation of the plasma membrane of the lumenal surface of rat bladder epithelium, and the occurrence of a hexagonal lattice of subunits both in negatively stained whole mounts and in sectioned membranes. *J. Cell Biol.* **45**:542.
12. Hlad, C. J., Jr., R. Nelson, and J. H. Holmes. 1956. Transfer of electrolytes across the urinary bladder in the dog. *Amer. J. Physiol.* **184**:406.
13. Karnovsky, M. J. 1965. A formaldehyde-glutaraldehyde fixative of high osmolality for use in electron microscopy. *J. Cell Biol.* **27**(2, Pt.2): 137 a. (Abstr.)
14. Karnovsky, M. J. 1967. The ultrastructural basis of capillary permeability studied with peroxidase as a tracer. *J. Cell Biol.* **35**:213.
15. Klug, A., and D. J. DeRosier. 1966. Optical filtering of electron micrographs: Reconstruction of one-sided images. *Nature (London).* **212**:29.
16. Koss, L. G. 1969. The asymmetric unit membranes of the epithelium of the urinary bladder of the rat. *Lab. Invest.* **21**:154.
17. Luft, J. H. 1961. Improvements in epoxy resin embedding methods. *J. Biophys. Biochem. Cytol.* **9**:409.
18. Moor, H., and Mühlethaler. 1963. Fine structure in frozen-etched yeast cells. *J. Cell Biol.* **17**:609.
19. Porter, K. R., and M. A. Bonneville. 1963. An Introduction to the Fine Structure of Cells and Tissues. Lea and Febiger, Philadelphia.
20. Porter, K. R., K. R. Kenyon, and S. Badenhausen. 1965. Origin of discoidal vesicles in cells of transitional epithelium. *Anat. Rec.* **151**: 401a. (Abstr.)
21. Porter, K. R., K. Kenyon, and S. Badenhausen. 1967. Specializations of the unit membrane. *Protoplasma.* **63**:262.
22. Reynolds, E. S. 1963. The use of lead citrate at high pH as an electron-opaque stain in electron microscopy. *J. Cell Biol.* **17**:208.
23. Staehelin, L. A., F. J. Chlapowski, and M. A. Bonneville. 1970. Lumenal plasma membrane of the urinary bladder. I. Three-dimensional reconstruction from freeze-etch images. *J. Cell Biol.* **47**(2, Pt.2):200 a. (Abstr.)
24. Vergara, J., W. Longley, and J. D. Robertson. 1969. A hexagonal arrangement of subunits in membrane of mouse urinary bladder. *J. Mol. Biol.* **46**:593.
25. Warren, R. C., and R. M. Hicks. 1970. Structure of the subunits in the thick lumenal membrane of rat urinary bladder. *Nature (London).* **227**:280.